Oscillating Wings and Bodies with Flexure in Supersonic Flow

D. D. Liu,* P. Garcia-Fogeda,† and P. C. Chen‡
Arizona State University, Tempe, Arizona

The development of the Harmonic Gradient Method (HGM) and the Harmonic Potential Panel (HPP) method for nonplanar wings and bodies in unsteady supersonic flow is presented. They are proved to be accurate and versatile tools for computations of unsteady aerodynamics. According to a consistent formulation, the bases of both methods are now unified. Owing to the Harmonic Potential model, the optimal number of panels can be achieved without loss of computational accuracy, and, yet, it is least affected by the given Mach number and reduced frequency. Moreover, these methods are completely general in terms of input oscillatory frequencies, mode shapes, and body or planform geometries. To validate the HGM/HPP computer codes, various computed results are compared with several known cases. These results demonstrate that the computer codes are attractive in their efficiency and cost-effectiveness for aeroelastic analyses, which suggests immediate industrial applications.

Introduction

WITH the advent of supersonic aircraft and modern launch vehicles, there exists a need for an accurate airload prediction method for aeroelastic design analysis. While current methodology for interfering lifting surfaces in the subsonic regime is better established because of the development of the Doublet Lattice Method,[1] an equally effective supersonic method has been lacking for several decades. Many attempts have been made in recent years for development of such an effective method for the treatment of interfering configurations (e.g., Refs. 2-6). Most of the investigators followed Jones and Appa's Potential Gradient Method and modified it further. By contrast, the Harmonic Gradient Method,[5] (HGM) developed in 1983, encompasses a generalized formulation for nonplanar lifting surfaces, and, with that, it also achieves the requirements of computational accuracy and cost effectiveness. Among these attempts, the HGM appears to be one of the most promising methods to date. In fact, since 1983, several aircraft industries have already adopted the HGM for supersonic aeroelastic applications. To continue the development of the HGM, our current efforts have been engaged in the generalization of this method for axisymmetric bodies with flexure,[7,8] with a view towards a comprehensive program for computations of body-wing aerodynamics. In this paper, developments of the HGM and the Harmonic Potential Panel method (HPP) in the problem areas for wings and bodies will be addressed.

The essence of the HGM and the HPP method lies in the introduction of the Harmonic Potential (HP) model. With this model, substantial savings in the wing panel numbers can be achieved without the loss of computation accuracy. Furthermore, both HGM and the HPP codes are completely general in terms of the input wing/body geometry, mode-shapes and reduced frequencies. The ease of application of these codes is comparable to that of the Doublet Lattice Code or the USSAERO Code.[9] With these features, both codes combined can be attractive in that they can perform cost-effective analyses for complex aircraft configurations.

Meanwhile, the confidence level of these program codes depends largely on the results of validation. For this reason, various computed results of wings and bodies will be presented for verification with several known cases.

Presented as Paper 86-2.9.5 at the 15th Congress/International Council of the Aeronautical Sciences, London, England, Sept. 7-12, 1986; received Dec. 16, 1986; revision received Dec. 28, 1987.

*Associate Professor, Department of Mechanical and Aerospace Engineering. Member AIAA.
†Faculty Associate, Department of Mechanical and Aerospace Engineering. Member AIAA.
‡Graduate Student, Department of Mechanical and Aerospace Engineering. Member AIAA.

General Formulation

Let $\sigma = 0$ represent the wing formulation and $\sigma = 1$ the body. The perturbed potential integral can be written in general as

$$\phi_\sigma(x_0,y_0,z_0) = I_\sigma\left[F_\sigma\left(\frac{\partial}{\partial n}\right)^\sigma H\right] \tag{1}$$

where

$$I_o[\cdot] = \iint[\cdot]\mathrm{d}x\,\mathrm{d}y \text{ and } I_1[\cdot] = \int[\cdot]\mathrm{d}x$$

F_0 and F_1 are the doublet strengths for the wing and the body, respectively. The kernel function reads

$$H(x-x_0,\, y-y_0,\, z-z_0) = \frac{\cos\dfrac{\mu R}{M_\infty}}{R} e - i\mu(x-x_0) \tag{2}$$

where

$$R = \sqrt{(x-x_0)^2 - \beta^2((y-y_0)^2 + (z-z_0)^2)},\ \mu = kM_\infty^2/\beta^2$$

M_∞ is the freestream Mach number $\beta^2 = M_\infty^2 - 1$, and k is the reduced frequency.

On the surfaces of the wing and along the body axis, the doublet strengths of each panel can be expressed in terms of $a_{\sigma i}$, which can be obtained by solving the flow tangency equation on the panel surfaces,

$$[A_{\sigma ij}]\,\{a_{\sigma i}\} = \left\{\frac{\mathrm{D}h_{\sigma j}}{\mathrm{D}t}\right\} \tag{3}$$

where $A_{\sigma ij}$ represents the aerodynamic influence coefficient of the j-th panel to the i-th control point. $\mathrm{D}h_{\sigma j}/\mathrm{D}t$ represents the downwash, in which $h_{\sigma j}$ is the displacement of the j-th panel.

The unsteady pressure coefficients are

$$c_p^0 = -2\left[\frac{\partial}{\partial x_0} + ik\right]\phi_0(x_0,y_0,z_0)\, e^{ikt} \tag{4a}$$

for the wing and

$$c_p^1 = c_{p_0} + \delta_0(\Delta c_p) \cos\theta\, e^{ikt} \tag{4b}$$

for the body where c_{p_0} is the mean-flow pressure and Δc_p represents the unsteady pressure due to a small amplitude δ_0. It should be noted that a_{oi} for the body depends on the mean-flow solution due to the nonvanishing of the body thickness. Consequently, Δc_p should also depend on the mean-flow pressure c_{p_0}. Since the wing thickness is approximated by a lifting surface, the a_{oi} and the unsteady pressure c_p^0 in Eqs. (3) and (4a) are decoupled from the mean-flow solution.

Steady-Flow Results

Swept Rectangular Wing

With the subsonic leading and trailing edges, the planform in Fig. 1 is an interesting case for result verifications. An exact solution obtained by Cohen[10] clearly indicates the wave-wave interaction feature of the problem (Fig. 2). Among others, previous attempts by Chipman[11] using improved Mach Box method, and by Ueda and Dowell[4] using Doublet Point method, have shown smearing of data around wave-wave finite discontinuities. To capture these discontinuities, it is essential to create irregular panels along the Mach wave cuts. One type of the panel arrangements used by HGM code are shown in Fig. 1b. With 196 panels, lifting pressures are computed at the spanwise locations of 48 and 72% as shown in Fig. 2a and 2b. In so doing, both weak and strong wave discontinuities are properly captured in regions inboard and outboard of the tip Mach line, as well prescribed by Cohen's exact results.

Nonlinear Solutions for Bodies

Results of linear and nonlinear versions of HPP Code are presented in Fig. 3 and 4. Based on Van Dyke's iterative procedure[12] the HPP nonlinear code has been developed recently[8] to account for the nonlinear body thickness effects. It is the first time that the panel method, using the technique of particular solutions, is employed to treat the nonlinear problem without involving the field point computations. In Fig. 3, HPP results (linear) and HPP nonlinear results are compared with those computed by USSAERO Code and by exact characteristics[13] for a 26% thick ogive body at $M_\infty = 2.0$. The HPP nonlinear results compare very well with those computed by the method of exact characteristics. It is seen that the nonlinear effect due to thickness is substantial from apex to the midbody. Next, the nonlinear iterative scheme is applied to a 16% thick ogive-cylinder-boattail body at $M_\infty = 3.0$ and placed at an angle of attack $\alpha_0 = 3.2$ deg. Again, very good correlations are found with the computed results of the Parabolized Navier-Stokes (PNS) Code and the Euler Code.[14] Considerable deviations between the linear and the nonlinear results are again observed particularly on the windward side of the ogive part. It is believed that as long as the flow remains attached, the present HPP nonlinear method should yield results in favorable agreement with those obtained by computational methods in the supersonic Mach number range.

Stability Derivatives

Delta Wing

For the panel arrangement shown in Fig. 5, the large aspect ratio of each panel element in the proximity of wing tips of a 45 deg swept delta wing would have ordinarily caused numerical errors. To show that such is not the case for the HGM, we compare present HGM results with Mile's exact solution[15] in terms of damping-in-pitch lift and moment coefficients. It is seen that all are in very good agreement with the exact results. This implies that the HGM scheme used is a robust one in that the computed result is unaffected by the assigned panel shapes and sizes.

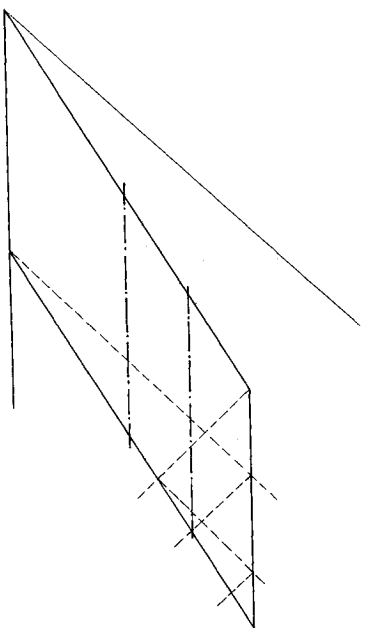

Fig. 1a Planform scheme for a swept rectangular wing.

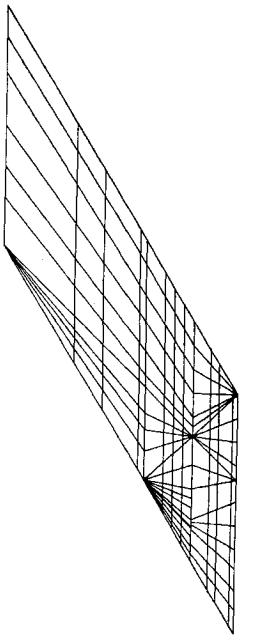

Fig. 1b Paneling scheme for a swept rectangular wing.

Ogive-Cylinder Body

It can be seen that in Fig. 6 the damping-in-pitch moments as computed by the present HPP methods are in fair agreement with the measured data[16] for a 20% thick ogive-cylinder body throughout the Mach number range. The computed results of Ref. 17 (SPINNER Code) and Ref. 18 show discrepancies with measured data; little dependency on Mach number was found in these analyses. By contrast, strong Mach number dependency is shown in the results of the HPP Code. However, no appreciable difference is found between the HPP linear and nonlinear results for this case.

Harmonic Potential Model

To achieve computation accuracy and effectiveness for wings or bodies in high-frequency oscillations, it is essential to render the Doublet solution and its convective gradient uniformly valid throughout the frequency domain. This is to say that the Doublet strength in each panel can be maintained spatially harmonic. In so doing, the element size is made automatically compatible to the wave number generated along the chord. Hence, the solution obtained can be least affected by the panel length and the input frequency.

In terms of Eq.(3), the HP model amounts to representing the unknown strengths a_{oi} by

$$a_{oi} = (b_i + c_i\, x)e^{i\mu x} \tag{5}$$

Figure 7 shows the doublet potential $\Delta\phi$ (or F_0 asnd F_1) behaves according to Eq. (5). As a result, as few as 30 panels are needed for a single wing planform using regular paneling scheme and 20 panels for a single body in actual computation.[5,7] In an IBM 3081 computer, typically only 90 CPU s and 7 CPU s are required, respectively, for computations of unsteady pressures.

Full-Frequency Domain

With the HP model built in, the HGM and the HPP methods can handle oscillatory problems in the full frequency domain effectively. In the high-frequency range, accurate solutions can be obtained without increasing the number of panel elements. Figures 8 and 9 present the unsteady pressures at the root chord section of a high-aspect-ratio rectangular wing in pitching and in plunging motions, respectively. For verification, the reduced frequencies "k" selected lie in the

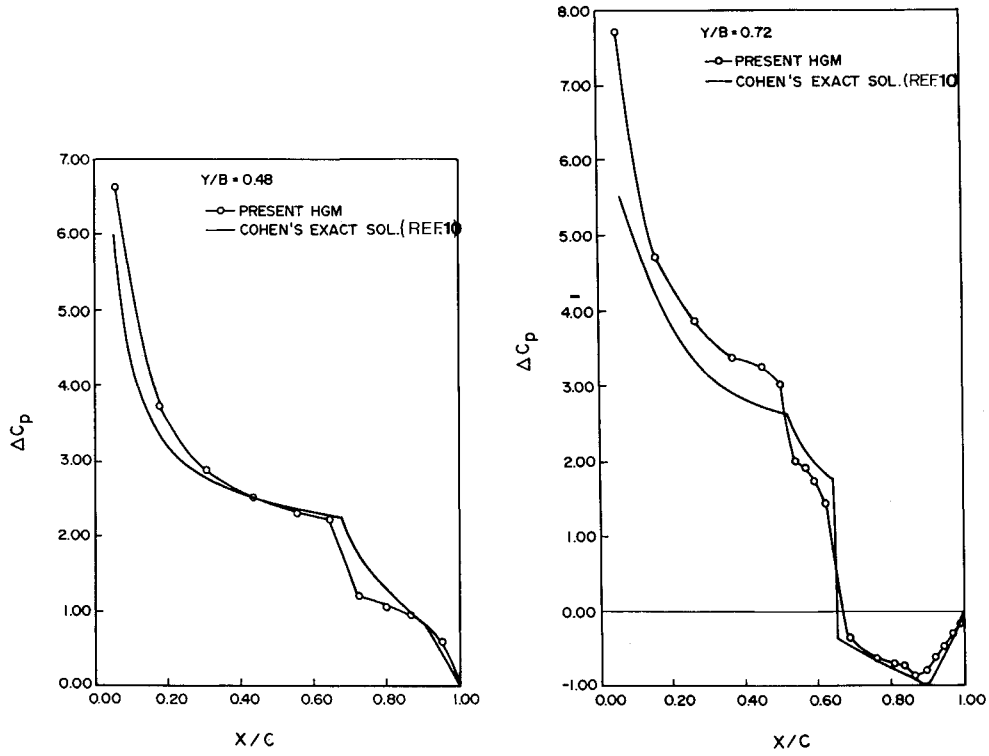

Fig. 2 Chordwise steady pressure distribution for swept rectangular wing at angle of attack.

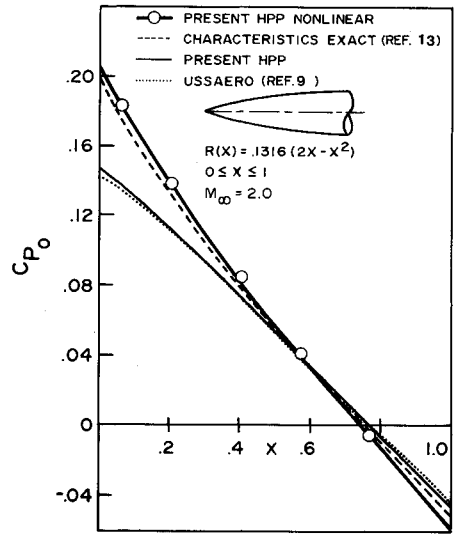

Fig. 3 Mean flow pressures for a parabolic-ogive at $M_\infty = 2.0$ and at angle of attack $\alpha_0 = 0$ deg.

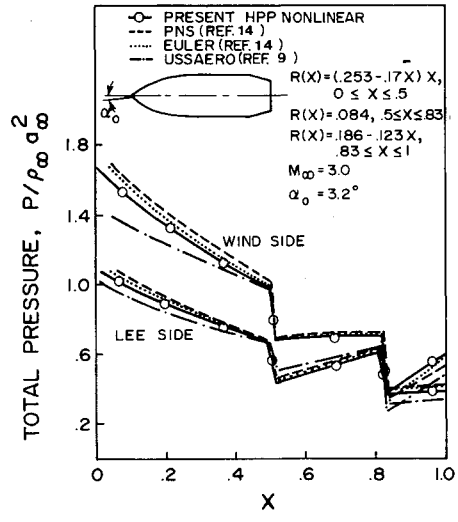

Fig. 4 Pressure distribution of an ogive-cylinder-boattail body at $M_\infty = 3.0$ and angle of attack $\alpha_0 = 3.2$ deg.

moderate to high range between 0.4 and 2.0 and the Mach numbers ($M_\infty = 1.15$ and 1.25) are selected in the lower range. As the root-chord is not contaminated by the tip Mach cone, it can be seen that the HGM results are in good agreement with several available two-dimensional results of Chadwick-Platzer[19] and of Liu and Pi[20] in Fig. 8, and with that of Jordan[21] in Fig. 9. For oscillating bodies, Fig. 10 presents results in the high-frequency limit. To validate the high-frequency solution of HPP Code, its computed results using 20 panel elements are checked against results calculated based on the piston theory for a very slender parabolic ogive. The thickness ratio $\tau = 0.02$ is selected according to the requirement of $\tau M_\infty k \ll 1$ as imposed by the piston theory. At $M_\infty = 1.5$, it is seen that agreement seems to be very good for two selected frequencies $k = 4.0$ and $k = 7.5$. It is also interesting to compare the effects of frequency and flow dimensionality on unsteady pressures. Figure 11 shows comparisons of unsteady pressure coefficients for a 5.7 deg cone and a flat plate pitching about the apex at $M_\infty = 2.0$. The HPP results are compared with the LPP results,[20] which are identical with the HGM results for a rectangular wing at the root chord. As expected, the unsteady pressure magnitudes for an oscillating cone are smaller than those of a flat plate at $k = 1.0$ and $k = 2.0$. Similar to the case of steady supersonic cone and wedge flows, the present finding shows that the cone in oscillation yields weaker compressions as a result of three dimensionality of the flow, irrespective of the oscillation frequency.

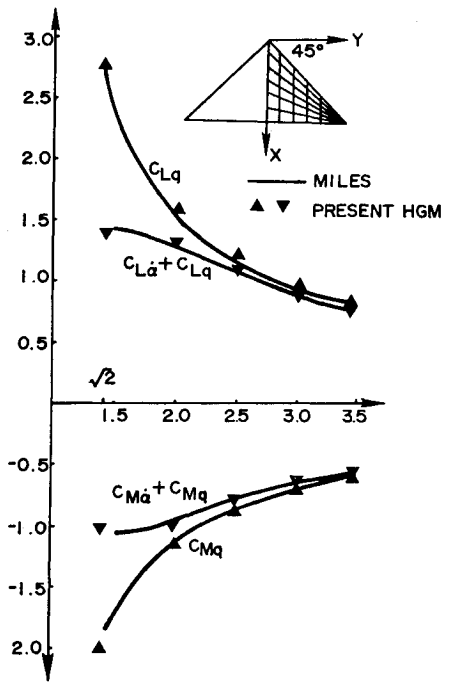

Fig. 5 Stability derivatives of a 45 deg delta wing at various Mach numbers.

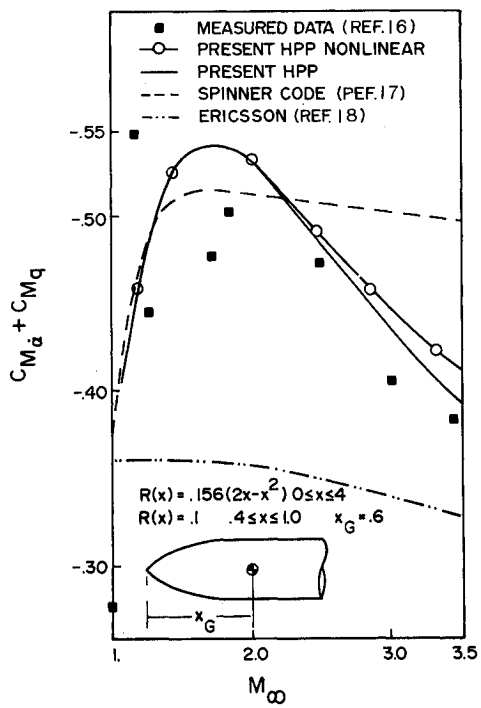

Fig. 6 Damping-in-pitch moment coefficient for a parabolic-ogive-cylinder at various Mach numbers.

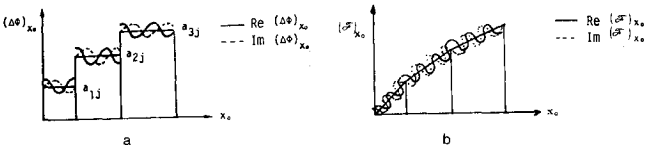

Fig. 7a Modeling of doublet strength: Harmonic Gradient Model (wing).

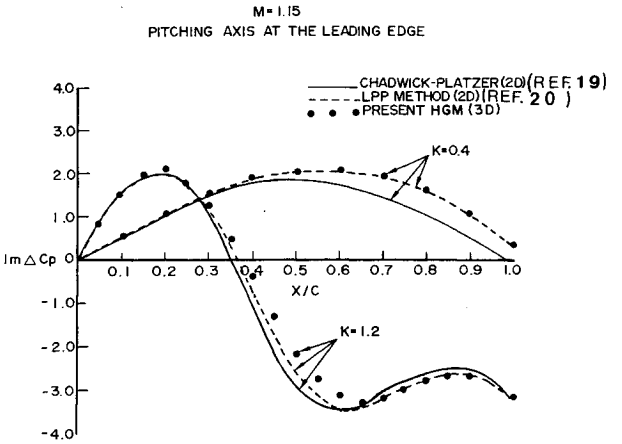

Fig. 7b Modeling of doblet strength; Harmonic Pontential Panel Model (body).

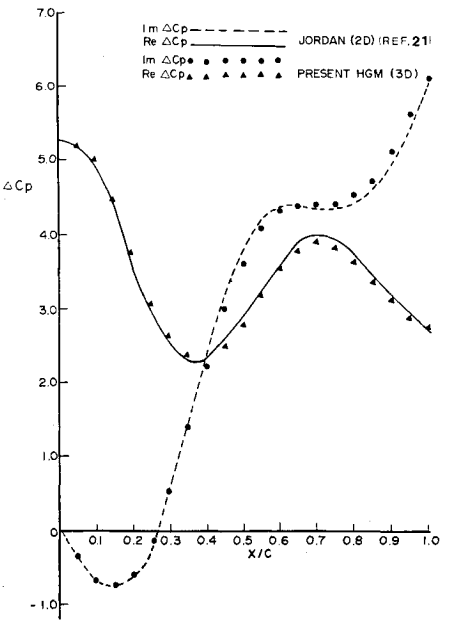

Fig. 8 Comparison of unsteady pressures with various two-dimensional methods at $M_\infty = 1.15$, $k = 0.4$ and $k = 1.2$. Pitching axis at the leading edge.

Oscillating Flexible Bodies

Coordinate Systems

It has been observed that a slender missile is susceptible to flutter when it is under a combination of short-period rigid mode and free-free bending mode oscillation during its supersonic flight phase.[22] To analyze such problems requires the proper selection of the coordinate systems. This question has been studied in depth by Garcia-Fogeda and Liu.[7] Basically, there are three coordinate systems to be considered: the wind-fixed, the body-fixed, and the pseudo-body-fixed (known as the pseudo-wind-fixed in Ref. 7; see Fig. 12). The first two systems have been subject to some controversy in the past.[23-26] It was found in Ref. 7 that, if ill formulated, the wind-fixed system will yield solutions that are generally singular at the body apex and at the body slope discontinuities. On the other hand, based on Van Dyke's first-order theory, a generalization to unsteady flow in the body-fixed system can be readily formulated to facilitate present studies. The pseudo-body-fixed coordinate system is a hybrid approximation between the first two systems. Its formulation is physically correct but not rigorous.

Bending Oscillations

In Fig. 13, computed HPP results for an elastic cone-cylinder body, oscillating in first bending mode, were compared with the aerodynamic damping data measured by Hanson and Doggett[27] for verification. The damping reduced frequency lies between 1.12 to 1.6, corresponding to $M_\infty = 3.0$ to 1.5. It is seen that the present results establish close trends to the measured data. By contrast, all quasisteady theories[12,33,34] yield much inferior predictions. It should be mentioned that equally close trends to the measured data were also predicted for the case of second-order, bending-mode oscillations.

Divergence and Flutter

The main application of the HGM and the HPP Codes lies in aeroelastic analyses such as the predictions of divergence and flutter boundaries. To verify these boundaries with measured data for wing planforms is difficult, as the latter are mostly kept out of the public domain. However, it should be noted that the HGM Code is presently used by several aircraft industries for flutter clearance purposes, as well as flutter predictions in their aeroelastic optimization program. Also, limited amount of flutter data is found to exist for bodies.

In Figs. 14 and 15, an oscillating cone of semiangle 7.5 deg in rigid mode at wind-off frequency ratio of $\omega_H/\omega_\alpha = 1.8$ is studied for divergence and flutter. The present HPP (linear) method and the HPP nonlinear method are used to compute the divergence and flutter boundaries. Here, the HPP nonlinear code is referred to a scheme using the nonlinear mean-flow solutions for unsteady flow computations (see Ref. 8). It is seen that consistent improvement in trend is obtained for the nonlinear results over the linear ones in comparison with the measured data of Sewall, Hess and Watkins,[28] whereas two of the quasisteady methods[35,36] fail to predict such a trend. However, the predicted boundaries become less conservative in the order of slender-body, the HPP-linear, and the HPP-nonlinear results. Little Mach number dependency is shown for the divergence boundary as predicted by the HPP nonlinear code up to $M_\infty = 5.0$. In Fig. 15, it is seen that overall trends of the predicted flutter speeds are comparable to those measured. Since the cone is a slender one, the predicted flutter speeds by the linear and the nonlinear methods merge in the low Mach number range as expected. A similar trend can be observed in the pressure distributions for the mean-flow cases.[12] It should be noted that, for thicker bodies, the linear and nonlinear results are expected to deviate from each other, as indicated by Van Dyke for the mean-flow cases.

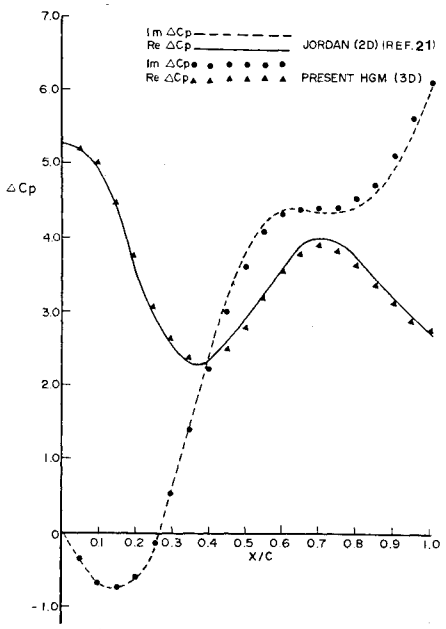

Fig. 9 Comparison of unsteady pressures at the root of a plunging high aspect ratio rectangular wing with Jordan's two-dimensional method at $M_\infty = 1.25$ and $k = 2.0$.

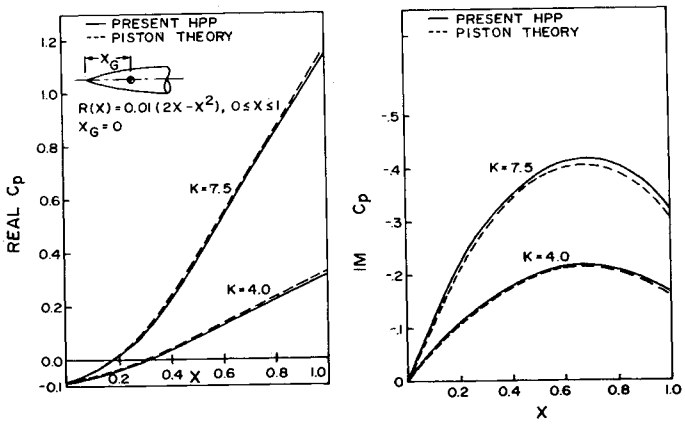

Fig. 10 In-phase and out-of-phase pressure coefficients for a parabolic-ogive in pitching mode at $M_\infty = 1.5$ and high reduced frequencies.

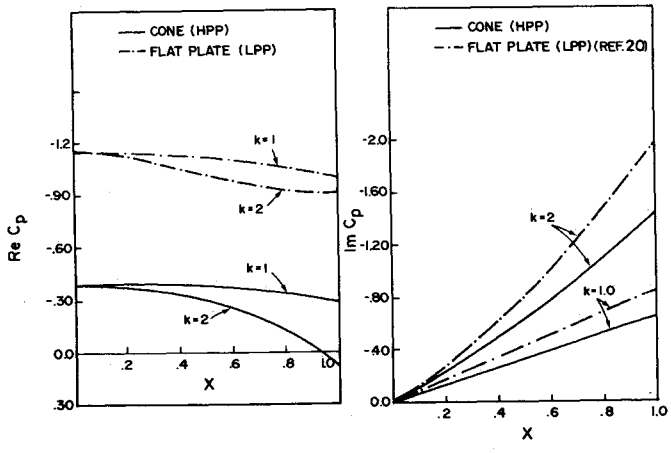

Fig. 11 Comparison of the in-phase and out-of-phase pressure coefficients at $M_\infty = 2.0$ for a 5.7 deg cone and a flat plate pitching at the apex.

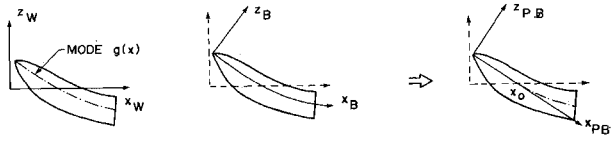

Fig. 12 Various coordinate systems for oscillating bodies.

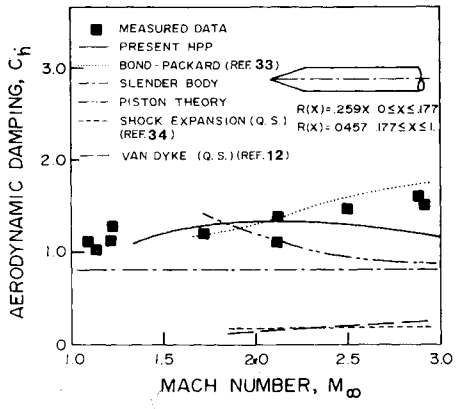

Fig. 13 Aerodynamic damping coefficients vs Mach number for a cone-cylinder vibrating in first bending mode.

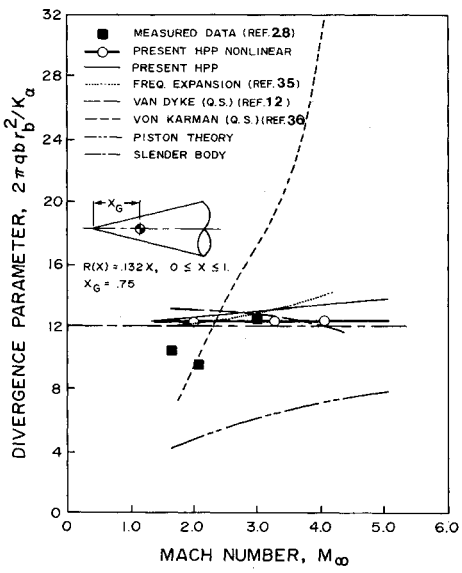

Fig. 14 Divergence boundaries vs Mach number for a 7.5 deg cone.

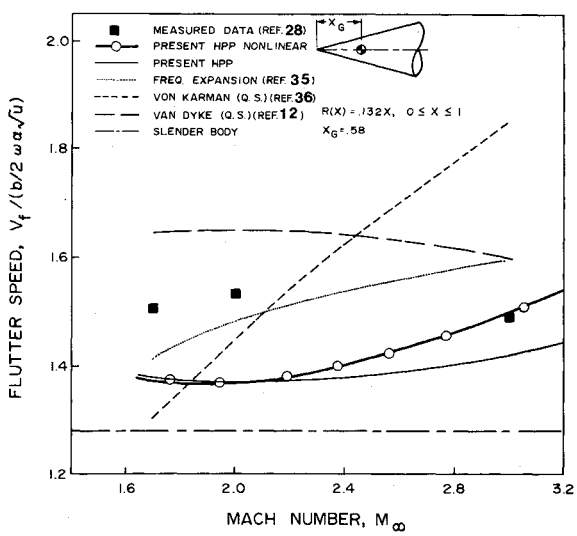

Fig. 15 Flutter speed boundaries vs Mach number for a 7.5 deg cone.

Other Configurations

Saturn Launch Vehicle

In Fig. 16, aerodynamic damping of the Saturn SA-1 launch vehicle is presented. To compare with Hanson and Doggett's measured data,[29] the free-free first bending mode and damping frequencies as determined by the experiment are used as the inputs for the present HPP Code. The natural frequency for the actual vehicle is 2.8 Hz; however, for wind tunnel experiments, the model natural frequency is 153 Hz due to the necessary scale-down in size. Consequently, the reduced frequency lies between 1.4 to 2.53 for Mach number range between 3.0 to 1.2, respectively. Thus, the reduced frequency range for the model study is of order unity. This justifies the necessity of a general method, such as the present HPP method that is valid in the full-frequency domain. Good agreements are seen between present results and the measured data. To model this complex configuration, less than 100 panels are used with the given frequency range. Only 30 s CPU time on an IBM 3081 computer were needed for computing the aerodynamic damping coefficient for one freestream Mach number.

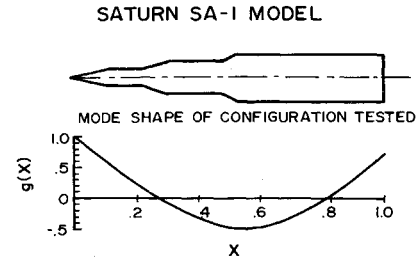

GEOMETRY OF THE CONFIGURATION

R(X)=.2296X	0 ≤ X ≤ .1317
R(X)=.03024	.1317 ≤ X ≤ .241
R(X)=.268X-.03445	.241 ≤ X ≤ .3353
R(X)=.05541	.3353 ≤ X ≤ .5066
R(X)=.4515X-.17332	.5066 ≤ X ≤ .5288
R(X)=.06543	.5288 ≤ X ≤ 1.0

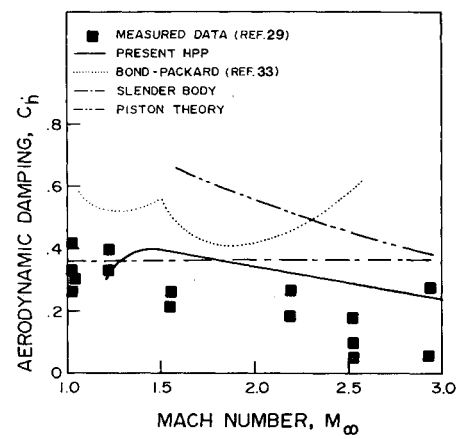

Fig. 16 Comparison of computed and experimental aerodynamic damping coefficients vs Mach number for a Saturn SA-1 configuration vibrating in first bending mode.

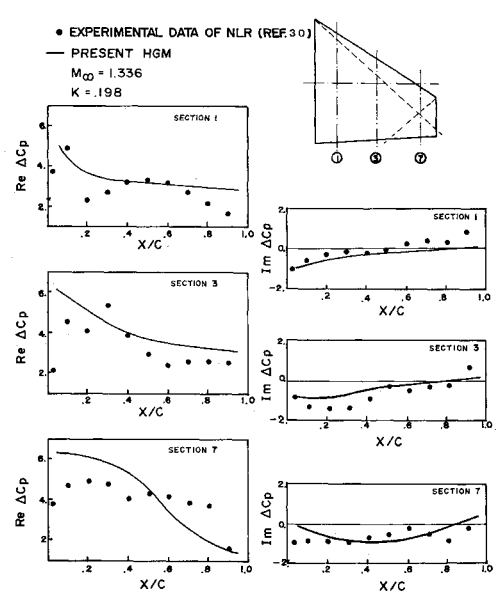

Fig. 17 Comparison of computed unsteady pressure on a Northrop F-5 wing with experimental data of NLR: 1 $Y/B = 18\%$; sect. 3 $Y/B = 51.2\%$; sect. 7 $Y/B = 87.5\%$.

Northrop F-5 Wing

Tijdeman et al.[30] at NLR have performed a series of experiments on a pitching F-5 wing throughout the whole transonic range. We select the highest Mach number case in this series ($M_\infty = 1.336$) for the computation example presented in Fig. 17. With the pitching axis located at 50% of the root chord, the wing is pitching at a frequency of $k = 0.198$. Sections 1, 3, and 7 are selected, which are located at 18%, 51.2% and 87.5% of the semispan, respectively.

The HGM code computes this case without the scheme of the Mach wave cut. Ten chordwise and 12 spanwise panels are uniformly distributed on the wing surface. It is seen that the correlations between the computed results and the measured data are fair. The reason for this is that physically there exists strong influence of the nonlinear effect due to a detached shock wave near the leading edge, whereas the HGM is a linear method. Also observed is the oscillatory feature of the measured data. The cause of this feature in the measured data is not totally clear. We believe that the oscillatory pressure in this flow regime could in turn affect the flutter results to a certain extent. Investigation of this problem requires the careful study of the nonlinear transonic/supersonic flow at the near shock-attachment or detachment conditions. Such a study is currently in progress.

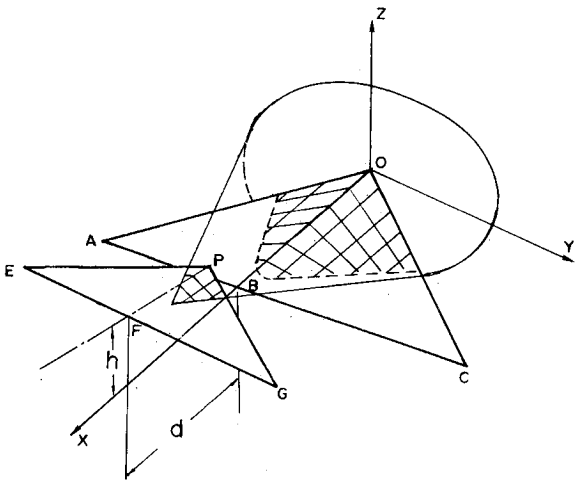

Fig. 18 Nonplanar wing-tail configuration showing notations ($OB = 2\sqrt{3}$, $PF = \sqrt{3}/2$, $AC = 4$ and $EG = 2$).

Nonplanar Wings

Computations were carried out for a wing and a tailplane, both with delta planforms in tandem configuration, as shown in Fig. 18. Two coplanar cases and three nonplanar cases are considered according to Woodcock and York.[31] The fixed geometric parameters for this arrangement are

$$\text{root chords:} \quad OB = 2\sqrt{3} \text{ and } PF = \sqrt{3}/2$$
$$\text{wing spans:} \quad AC = 4 \text{ and } EG = 2,$$

whereas the varied parameters are d, the distance between the wing and the tail measured along the x-axis from one trailing edge to the other, and h, the height between the mean planes of the wing and the tail. Case 2 and case 5 are two special cases. In case 2, the coplanar wing and tail join at point B (also now point P); in case 5, no interference occurs between the two surfaces.

Four modes were considered:
mode 1: both wing and tail in plunging motion,
mode 2: both wing and tail in pitching motion,
mode 3: the tail alone in plunging motion, and
mode 4: the tail alone in pitching motion,

while the pitch axis remains fixed at two thirds of the wing root chord for all modes.

The generalized forces should read

$$\rho_\infty U_\infty^2 L^2 S(Q'_{IJ} + ik\, Q''_{IJ})$$

where L is the reference chord length, S is the reference span length and k the reduced frequency, and they are set to $\sqrt{3}$, 2, and 0.01, respectively, for the present cases.

Only the out-of-phase part of the generalized forces, Q''_{IJ}, is presented in Tables 1 and 2. Computed results of HGM are compared with those by Woodcock and York using the Box Collocation method and by an approximate method of Martin et al.[32] Close agreement with Woodcock's results are found for the coplanar cases. For the nonplanar cases, some deviations are found in the values of Q''_{12}, Q''_{21}, Q''_{31}, and Q''_{41}.

It should be noted that the present HGM adopts a total of 125 panels, 100 for the wing and 25 for the tail, whereas Woodcock uses 350 boxes. In our earlier work,[5] as few as 50 panels were used to compute for an AGARD Wing-Tail-Fin combination. Little difference was found in the generalized forces between using 100 panels and 50 panels to represent the cases of wing-tail and fin-tail interferences.

Table 1 Out-of-phase generalized forces for coplanar tandem-wing interference, $M_\infty = 1.44$, $k = 0.01$.

	Case 1 $d = 2.866$ $h = 0$			Case 2 $d = 0.866$ $h = 0$		
Q''_{IJ}	HGM	Woodcock[31]	Martin[32]	HGM	Woodcock[31]	Martin[32]
11	3.073	2.951	2.99	3.160	2.88	3.06
12	1.439	1.473	1.43	0.348	0.20	0.37
13	0.489	0.469	– –	0.489	0.477	– –
14	0.997	0.925	– –	0.432	0.387	– –
21	0.345	0.326	0.32	0.259	0.110	0.21
22	4.102	4.142	4.40	1.104	0.970	1.70
23	1.055	1.016	– –	0.490	0.483	– –
24	2.154	2.007	– –	0.437	0.395	– –
31	0.151	0.149	– –	0.238	0.07	– –
32	1.646	1.635	– –	0.555	0.37	– –
33	0.489	0.469	– –	0.489	0.477	– –
34	0.997	0.925	– –	0.432	0.387	– –
41	0.324	0.321	– –	0.238	0.09	– –
42	3.562	3.553	– –	0.563	0.40	– –
43	1.055	1.016	– –	0.490	0.483	– –
44	2.154	2.007	– –	0.437	0.395	– –

Table 2 Out-of-phase generalized forces for nonplanar tandem-wing interference, $M_\infty = 1.44$, $k = 0.01$.

	Case 3 $d = 0.866$ $h = 0.5$		Case 4 $d = 0.866$ $h = 1.0$		Case 5 $d = 0.866$ $h = 5.0$	
Q''_{IJ}	HGM	Woodcock[31]	HGM	Woodcock[31]	HGM	Woodcock[31]
11	3.161	2.965	3.065	3.028	3.412	3.282
12	0.264	0.170	0.269	0.141	0.225	0.214
13	0.489	0.477	0.489	0.477	0.489	0.477
14	0.432	0.387	0.432	0.387	0.432	0.387
21	0.272	0.171	0.164	0.240	0.512	0.499
22	1.026	0.934	1.018	0.896	0.977	0.971
23	0.490	0.483	0.490	0.483	0.490	0.483
24	0.437	0.395	0.437	0.395	0.437	0.395
31	0.239	0.148	0.142	0.222	0.489	0.477
32	0.471	0.343	0.476	0.315	0.432	0.387
33	0.489	0.477	0.489	0.477	0.489	0.477
34	0.432	0.387	0.432	0.387	0.432	0.387
41	0.250	0.155	0.112	0.224	0.490	0.483
42	0.485	0.358	0.478	0.319	0.437	0.395
43	0.490	0.483	0.490	0.483	0.490	0.483
44	0.437	0.395	0.437	0.395	0.437	0.395

Conclusions

It has been shown that the present method has the following advantage over the existing unsteady supersonic methods:

1) The present method formulation is consistently based on the Harmonic Potential Model. It is general in the frequency domain and for arbitrary input mode shapes.

2) The present method is general for computing nonplanar or coplanar wing planforms, as well as for axisymmetric bodies with any given body shape, including slope discontinuities.

3) Due to the Harmonic Potential Model, the required number of panels is least affected by the given Mach number and reduced frequencies, and yet without the loss of computational accuracy.

4) Both HGM and HPP Codes are computationally efficient in terms of computing time. The ease of application of these codes is comparable to that of the subsonic Doublet Lattice Code. Therefore, we believe that a comprehensive, three-dimensional, unsteady, supersonic method for body-wing combinations is nearly in hand. With the above features, properly combining both codes into one can provide aircraft industries with a cost-effective tool in performing supersonic aeroelastic analyses for a complex aircraft configuration. We are presently continuing our effort towards this goal.

Acknowledgment

The present work is supported in part by the U.S. Army Research Office. The authors would like to thank Richard Chipman of Grumman Aerospace Corporation for valuable discussions and his suggestion of the swept-rectangular wing case.

References

[1]Rodden, W. P., Giesing, J. P., and Kalman, T. P., "New Developments and Applications of the Subsonic Doublet-Lattice Method for Non-planar Configuration," AGARD Symposium on Unsteady Aerodynamics for Aeroelastic Analyses of Interfering Surfaces, Paper 4, Tousberg Oslogjorden, Norway, Nov. 1970.

[2]Jones, W. P. and Appa, K., "Unsteady Supersonic Aerodynamic Theory for Interfering Surfaces by the Method of Potential Gradient," NASA CR-2898, 1977.

[3]Hounjet, M. H. L., "Improved Potential Gradient Method to Calculate Airloads on Oscillating Supersonic Interfering Surfaces," *Journal of Aircraft*, Vol. 19, May 1982, pp. 390–399.

[4]Ueda, T. and Dowell, E. H., "Doublet-Point Method for Supersonic Unsteady Lifting Surfaces," *AIAA Journal*, Vol. 22, Feb. 1984, pp. 179–186.

[5]Chen, P. C. and Liu, D. D., "A Harmonic Gradient Method for Unsteady Supersonic Flow Calculations," *Journal of Aircraft*, Vol. 22, May 1985, pp. 371–379.

[6]Zhang, F. Q. and Forsching, H., "An Improved Potential Gradient Method for the Calculation of Unsteady Aerodynamic Pressures on Oscillating Wings in Supersonic Flow," Paper 10, Second International Symposium on Aeroelasticity and Structural Dynamics, DGLR-Bericht 85-02, Aachen, FRG, April 1985, pp. 153–1862.

[7]Garcia-Fogeda, P. and Liu, D. D., "A Harmonic Potential Panel Method for Flexible Bodies in Unsteady Supersonic Flow," AIAA Paper 86-0007, Jan. 1986.

[8]Garcia-Fogeda, P. and Liu, D. D., "Aeroelastic Applications of Harmonic Potential Panel Method to Oscillating Flexible Bodies in Supersonic Flow," AIAA Paper 86-0864-CP, May 1986.

[9]Woodward, F. A., "An Improved Method for the Aerodynamic Analysis of Wing-Body-Tail Configurations in Subsonic and Supersonic Flow," NASA CR-2228, 1973.

[10]Cohen, D., "Formulas for the Supersonic Loading, Lift and Drag of Flat Swept-Back Wings with Leading Edges Behind the Mach Line," NACA Report 1050, 1951.

[11]Chipman, R., "An Improved Mach-Box Approach for Supersonic Oscillatory Pressures," *Journal of Aircraft*, Vol. 14, Sept. 1977, pp. 887–893.

[12]Van Dyke, M. D., "First and Second Order Theory of Supersonic Flow Past Bodies of Revolution," *Journal of Aeronautical Sciences*, Vol. 18, March 1951, pp. 161–178.

[13]Krasnov, N. F., *Aerodynamics of Bodies of Revolution*, American Elsevier Pub., New York, 1970, pp. 239–263.

[14]Schiff, L. B. and Sturek, W. B., "Numberical Simulation of Steady Supersonic Flow Over an Ogive-Cylinder-Boattail Body," AIAA Paper 80-0066, 1980.

[15]Miles, John W., *The Potential Theory of Unsteady Supersonic Flow*, Cambridge Univ. Press, UK, 1959, pp. 128–149.

[16]Uselton, B. L. and Shadow, T. O., "Dynamic Stability Characteristics of 3- and 5-Cal Army Navy Spinner Projectiles at Mach Numbers 0.2 through 1.3," AEDC-TR-70-115, July 1970.

[17]Whyte, R. H., "'Spinner'—A Computer Program for Predicting the Aerodynamic Coefficients of Spin-Stabilized Projectiles," G.E. Technical Information Service, Class 2, 69APB3, Aug. 1969.

[18]Ericsson, L. E., "Viscous Effects on Missile Aerodynamics at Low Angles of Attack," *Journal of Spacecraft and Rockets*, Vol. 18, Sept.–Oct. 1981, pp. 401–405.

[19]Chadwick, W. R., "Unsteady Supersonic Cascade Theory Including Nonlinear Thickness Effects," Ph.D. Thesis, Naval Postraduate School, Monterey, CA, June 1975; also AGARD CP-177, Sept. 1975.

[20] Liu, D. D. and Pi, W. S., "Transonic Kernel Function Method for Unsteady Flow Calculations Using a Unified Linear Pressure Panel Procedure," AIAA Paper 80-0737-CP.

[21]Jordan, P. F., "Aerodynamics Flutter Coefficients for Subsonic, Sonic and Supersonic Flow (Linear Two-Dimensional Theory)," Aeronautical Research Council RM 2932, 1957.

[22]Farrar, D. J., "Structures," *Journal of the Royal Aeronautical Society*, Vol. 60, Nov. 1956, pp. 712–720.

[23]Hoffman, G. and Platzer, M. F., "On Supersonic Flow Past Oscillating Bodies of Revolution," *AIAA Journal*, Vol. 4, Feb. 1966, p. 370.

[24]Labrujere, T. E., Roos, R., and Erkelens, L. J. J., "The Use of Panel Methods with a View to Problems in Aircraft Dynamics," NLR MP-77009U.

[25]Platzer, M. F. and Liu, D. D., "A Linearized Characteristics Method for Supersonic Flow Past Bodies of Revolution Performing Bending Oscillations," Report LMSC/HREC A784262, Lockheed Missiles and Space Co., Huntsville, AL, May 1967.

[26]Hoffman, G. H. and Platzer, M. F., "Higher Approximations for Supersonic Flow Past Slowly Oscillating Bodies of Revolution," *Acta Mechanica*, Vol. 5, 1968, pp. 143–162.

[27]Hanson, P. W. and Doggett, R. V., "Wind-Tunnel Measurements of Aerodynamic Damping Derivatives of a Launch Vehicle Vibrating in Free-Free Bending Modes at Mach Numbers from 0.70 to 2.87 and Comparisons with Theory," NASA TN D-1391, Oct. 1962.

[28]Sewall, J. L., Hess, R. W., and Watkins, C. E., "Analytical and Experimental Investigation of Flutter and Divergence of Spring-Mounted Cone Configurations at Supersonic Speeds," NASA TN D-1021, April 1962.

[29]Hanson, P. W. and Doggett, R. V., "Aerodynamic Damping of a 0.02-Scale Saturn SA-1 Model Vibrating in the First Free-Free Bending Mode," NASA TN D-1956, Sept. 1963.

[30]Tijdeman, "Transonic Wind Tunnel on an Oscillating Wing with External Store, Part II: The Clean Wing," NLR TR 78106, Pt II: also Air Force Flight Dynamics Lab., TR-78-194, May 1979, pp. 20–1 to 20–25.

[31]Woodcock, D. L. and York, E. J., "A Supersonic Box Collocation Method for the Calculation of Unsteady Airforces of Tandem Surfaces," AGARD-CP-80-71 Symposium on Unsteady Aerodynamics for Aeroelastic Analysis of Interfering Surfaces, Part I, Paper 6.

[32]Martin, J. C., Diederich, M. S., and Bobbit, P. J., "A Theoretical Investigation of the Aerodynamics of Wing-Tail Combinstions Performing Time-Dependent Motions at Supersonic Speeds," NACA TN 3072, 1954.

[33]Bond, R. and Packard, B. B., "Unsteady Aerodynamic Forces on a Slender Body of Revolution in Supersonic Flow," NASA TN D-859, May 1961.

[34]Syvertson, C. A. and Dennis, D. H., "A Second-Order Shock Expansion Method Applicable to Bodies of Revolution Near Zero Lift," NACA Report 1328, 1957.

[35]Lansing, D. L., "Velocity Potential and Forces on Oscillating Slender Bodies of Revolution in Supersonic Flow Expanded to the Fifth Power of the Frequency," NASA TN D-1225, 1962.

[36]von Kármán, T. and Morre, N. B., "The Resistance of Slender Bodies," *Transactions of the American Society of Mechanical Engineers*, Vol. 54, pp. 303–310.